

Vibration and stability of embedded cylindrical shell conveying fluid mixed by nanoparticles subjected to harmonic temperature distribution

Maryam Shokravi*¹ and Nader Jalili²

¹Buein Zahra Technical University, Buein Zahra, Qazvin, Iran

²Piezoactive Systems Laboratory, Department of Mechanical and Industrial Engineering, Northeastern University, Boston, Massachusetts 02115, USA

(Received May 20, 2017, Revised September 11, 2017, Accepted September 17, 2017)

Abstract. Nonlinear vibration and instability of cylindrical shell conveying fluid-nanoparticles mixture flow are studied in this article. The surrounding elastic medium is modeled by Pasternak foundation. Mixture rule is used for obtaining the effective viscosity and density of the fluid-nanoparticles mixture flow. The material properties of the elastic medium and cylindrical shell are assumed temperature-dependent. Employing first order shear deformation theory (FSDT), the motion equations are derived using energy method and Hamilton's principal. Differential quadrature method (DQM) is used for obtaining the frequency and critical fluid velocity. The effects of different parameters such as volume percent of nanoparticles, boundary conditions, geometrical parameters of cylindrical shell, temperature change, elastic foundation and fluid velocity are shown on the frequency and critical fluid velocity of the structure. Results show that with increasing volume percent of nanoparticles in the fluid, the frequency and critical fluid velocity will be increases.

Keywords: cylindrical shell; instability; fluid-nanoparticles mixture flow; temperature-dependent; DQM

1. Introduction

The mix of fluid and nanoparticles produces a nanofluid. In nanofluids, common base nanoparticles include metals, oxides, carbides, or carbon nanotubes. The main advantage of nanofluids is heat resistances which have many applications in fuel cells, hybrid-powered engines, chiller, heat exchanger, boiler and etc. Knowledge of the instability behaviour of nanofluids on the structures is found to be very critical in deciding their suitability for convective heat transfer applications.

There are many works in the literature for instability induced by fluid flow on different structures. Ryu *et al.* (2004) studied vibration and dynamic stability of cantilevered pipes conveying fluid on elastic foundations. Amabili (2008) studied vibration and stability of cylindrical shell conveying fluid using different theories. The instability of simply supported pipes

*Corresponding author, Ph.D., E-mail: Maryamshokravi10@yahoo.com; Maryamshokravi10@bzte.ac.ir

conveying fluid under thermal loads was studied by Qian *et al.* (2009). A relatively new semi-analytical method, called differential transformation method (DTM), was generalized by Ni *et al.* (2011) to analyze the free vibration problem of pipes conveying fluid with several typical boundary conditions. Instability of supported pipes conveying fluid subjected to distributed follower forces was investigated by Wang (2012) based on the Pflüger column model. Marzani *et al.* (2012) investigated the effect of a non-uniform Winkler-type elastic foundation on the stability of pipes conveying fluid fixed at the upstream end only. The dynamics of fluid-conveying cantilevered pipe consisting of two segments made of different materials was studied by Dai and Ni (2013), focusing on the effects induced by different length ratios between the two segments. An analytical study of the velocity profile effects for a straight pipe was presented by Kutin and Bajsić (2014). A numerical simultaneous solution involving a linear elastic model was applied by Sun and Gu (2014) to study the fluid-structure interaction (FSI) of membrane structures under wind actions. Based on Euler-Bernoulli beam theory, Dai *et al.* (2014) studied instability of tubes conveying fluid. The unsteady fluid-structure interaction (FSI) problems with large structural displacement were solved by He (2015) using partitioned solution approaches in the arbitrary Lagrangian-Eulerian finite element framework. Rivero-Rodriguez and Pérez-Saborid (2015) carried out a numerical investigation of the three dimensional nonlinear dynamics of a cantilevered pipe conveying fluid in the presence of gravity. Texier and Dorbolo (2015) described the deformation of an elastic pipe submitted to gravity and to an internal fluid flow. Maalawi *et al.* (2016) enhanced the pipe overall stability level and avoid the occurrence of flow. Ghaitani and Majidian (2017) addressed vibration and instability of embedded functionally graded (FG)-carbon nanotubes (CNTs)-reinforced pipes conveying viscous fluid. Structural model for a slender and uniform pipe conveying fluid, with axially moving supports on both ends, immersed in an incompressible fluid, was formulated by Ni *et al.* (2017). A hybrid method which combines reverberation-ray matrix method and wave propagation method was developed by Deng *et al.* (2017) to investigate the stability of multi-span viscoelastic functionally graded material (FGM) pipes conveying fluid.

Based on author knowledge, no report has been found on the instability of pipes conveying fluid-nanoparticles mixture. However, in this paper, vibration and instability of embedded cylindrical shell conveying fluid-nanoparticles mixture are studied. The material properties of cylindrical shell and elastic foundation are assumed temperature-dependent. Based on FSDT, energy method and Hamilton's principle, the motion equations are derived. Using DQM, the frequency and critical fluid velocity of the structure are obtained. The effects of volume percent of nanoparticles, boundary conditions, geometrical parameters of cylindrical shell, temperature change, elastic foundation and fluid velocity are shown on the frequency and critical fluid velocity of the structure.

2. Formulation

Fig. 1 shows a cylindrical shell conveying fluid mixed by nanoparticles with the radius of R , thickness of h , length of L , density of ρ . The elastic medium is modeled by the spring coefficient k_w and shear layer k_g .

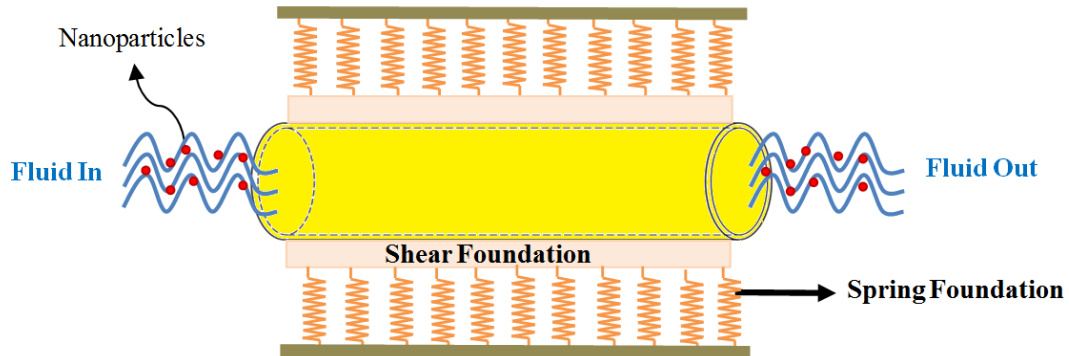


Fig. 1 Scheme of cylindrical shell conveying fluid mixed by nanoparticles surrounded by elastic medium

2.1 Strain-displacement relations

Based on FSDT shell theory, the displacement field can be expressed as (Reddy 2004)

$$u(x, \theta, z, t) = u(x, \theta, t) + z\phi_x(x, \theta, t), \tag{1}$$

$$v(x, \theta, z, t) = v(x, \theta, t) + z\phi_\theta(x, \theta, t), \tag{2}$$

$$w(x, \theta, z, t) = w(x, \theta, t), \tag{3}$$

where $(u(x, \theta, z, t), v(x, \theta, z, t), w(x, \theta, z, t))$ denote the displacement components at an arbitrary point (x, θ, z) in the shell, and $(u(x, \theta, t), v(x, \theta, t), w(x, \theta, t))$ are the displacement of a material point at (x, θ) on the mid-plane (i.e., $z=0$) of the shell along the x -, θ -, and z -directions, respectively; ϕ_x and ϕ_θ are the rotations of the normal to the mid-plane about x - and θ -directions, respectively. Based on above relations, the strain-displacement equations may be written as

$$\varepsilon_{xx} = \frac{\partial u}{\partial x} + z \frac{\partial \phi_x}{\partial x}, \tag{4}$$

$$\varepsilon_{\theta\theta} = \frac{1}{R} \left(w + \frac{\partial v}{\partial \theta} \right) + \frac{z}{R} \frac{\partial \phi_\theta}{\partial \theta}, \tag{5}$$

$$\gamma_{x\theta} = \frac{\partial v}{\partial x} + \frac{1}{R} \left(\frac{\partial u}{\partial \theta} \right) + z \left(\frac{\partial \phi_\theta}{\partial x} + \frac{1}{R} \frac{\partial \phi_x}{\partial \theta} \right), \tag{6}$$

$$\gamma_{xz} = \phi_x + \frac{\partial w}{\partial x}, \quad (7)$$

$$\gamma_{z\theta} = \frac{1}{R} \left(\frac{\partial w}{\partial \theta} - v \right) + \phi_\theta. \quad (8)$$

where $(\varepsilon_{xx}, \varepsilon_{\theta\theta})$ are the normal strain components and $(\gamma_{\theta z}, \gamma_{xz}, \gamma_{x\theta})$ are the shear strain components.

2.2 Stress-strain relations

The stress-strain relation can be written as

$$\begin{bmatrix} \sigma_{xx} \\ \sigma_{\theta\theta} \\ \sigma_{zz} \\ \tau_{\theta z} \\ \tau_{xz} \\ \tau_{x\theta} \end{bmatrix} = \begin{bmatrix} C_{11} & C_{12} & C_{13} & 0 & 0 & 0 \\ C_{12} & C_{22} & C_{23} & 0 & 0 & 0 \\ C_{13} & C_{23} & C_{33} & 0 & 0 & 0 \\ 0 & 0 & 0 & C_{44} & 0 & 0 \\ 0 & 0 & 0 & 0 & C_{55} & 0 \\ 0 & 0 & 0 & 0 & 0 & C_{66} \end{bmatrix} \begin{bmatrix} \varepsilon_{xx} - \alpha_{xx} T \\ \varepsilon_{\theta\theta} - \alpha_{\theta\theta} T \\ \varepsilon_{zz} - \alpha_{zz} T \\ \gamma_{\theta z} \\ \gamma_{xz} \\ \gamma_{x\theta} \end{bmatrix}, \quad (9)$$

where C_{ij} ($i, j=1, 2, \dots, 6$) denotes elastic coefficients; $\alpha_{xx}, \alpha_{\theta\theta}$ are thermal expansion and T is temperature rise which follows from a sinusoidal law as

$$T(z) = \Delta T \left(1 - \cos \left[\frac{\pi}{2} \left(\frac{z}{h} + \frac{1}{2} \right) \right] \right) + T_i, \quad \Delta T = T_o - T_i. \quad (10)$$

2.3 Energy method

2.3.1 Potential energy

The potential energy of the structure is

$$U = \frac{1}{2} \int (\sigma_{xx} \varepsilon_{xx} + \sigma_{\theta\theta} \varepsilon_{\theta\theta} + \tau_{xz} \gamma_{xz} + \tau_{\theta z} \gamma_{\theta z} + \tau_{x\theta} \gamma_{x\theta}) dV \quad (11)$$

Replacing the strain-displacement equations in the above relationships, we have

$$U = \frac{1}{2} \int_0^{2\pi} \int_0^L \left\{ \left[N_{xx} \frac{\partial u}{\partial x} + M_{xx} \frac{\partial \phi_x}{\partial x} \right] + \left[\frac{N_{\theta\theta}}{R} \left(w + \frac{\partial v}{\partial \theta} \right) + \frac{M_{\theta\theta}}{R} \frac{\partial \phi_\theta}{\partial \theta} \right] + Q_x \left(\phi_x + \frac{\partial w}{\partial x} \right) \right. \\ \left. + \left(N_{x\theta} \left[\frac{\partial v}{\partial x} + \frac{1}{R} \frac{\partial u}{\partial \theta} \right] + M_{x\theta} \left[\frac{\partial \phi_\theta}{\partial x} + \frac{1}{R} \frac{\partial \phi_x}{\partial \theta} \right] \right) + Q_\theta \left[\frac{1}{R} \left(\frac{\partial w}{\partial \theta} - v \right) + \phi_\theta \right] \right\} R dx d\theta, \quad (12)$$

where the stress resultant-displacement relations are as below

$$\begin{Bmatrix} N_x, M_x \\ N_\theta, M_\theta \\ N_{x\theta}, M_{x\theta} \end{Bmatrix} = \int_{-\frac{h}{2}}^{\frac{h}{2}} \begin{Bmatrix} \sigma_x \\ \sigma_\theta \\ \tau_{x\theta} \end{Bmatrix} (1, z) dz, \tag{13}$$

$$\begin{Bmatrix} Q_x \\ Q_\theta \end{Bmatrix} = k' \int_{-\frac{h}{2}}^{\frac{h}{2}} \begin{Bmatrix} \tau_{xz} \\ \tau_{\theta z} \end{Bmatrix} dz \tag{14}$$

In which k' is shear correction coefficient.

2.3.2 Kinetic energy

The kinetic energy of the structure can be written as

$$K = \frac{\rho}{2} \int \left(\left(\frac{\partial u}{\partial t} + z \frac{\partial \phi_x}{\partial t} \right)^2 + \left(\frac{\partial v}{\partial t} + z \frac{\partial \phi_\theta}{\partial t} \right)^2 + \left(\frac{\partial w}{\partial t} \right)^2 \right) dV. \tag{15}$$

where ρ is the density of the structure. Defining the moments of inertia as below

$$\begin{Bmatrix} I_0 \\ I_1 \\ I_2 \end{Bmatrix} = \int_{-h/2}^{h/2} \begin{Bmatrix} \rho \\ \rho z \\ \rho z^2 \end{Bmatrix} dz, \tag{16}$$

the kinetic energy may be written as

$$K = \frac{1}{2} \int \left(I_0 \left(\left(\frac{\partial u}{\partial t} \right)^2 + \left(\frac{\partial v}{\partial t} \right)^2 + \left(\frac{\partial w}{\partial t} \right)^2 \right) + I_1 \left(2 \frac{\partial u}{\partial t} \frac{\partial \phi_x}{\partial t} + 2 \frac{\partial v}{\partial t} \frac{\partial \phi_\theta}{\partial t} \right) + I_2 \left(\left(\frac{\partial \phi_x}{\partial t} \right)^2 + \left(\frac{\partial \phi_\theta}{\partial t} \right)^2 \right) \right) dA, \tag{17}$$

2.3.3 External work

The external work is due to the elastic foundation and fluid.

➤ **Elastic medium**

The external work due to the elastic medium is (Shokravi 2017a)

$$W_e = - \int (k_w w - k_g \nabla^2 w) w dA, \tag{18}$$

in which k_w and k_g are the spring and shear constants, respectively.

➤ **Fluid**

The external work caused by the fluid pressure is written as (Wang 2012)

$$W_f = \int (F_{fluid}) w dA = \int \left(-\rho_E A \left(\frac{\partial^2 w}{\partial t^2} + 2v_x \frac{\partial^2 w}{\partial x \partial t} + v_x^2 \frac{\partial^2 w}{\partial x^2} \right) + \mu A \left(\frac{\partial^3 w}{\partial x^2 \partial t} + \frac{\partial^3 w}{R^2 \partial \theta^2 \partial t} + v_x \left(\frac{\partial^3 w}{\partial x^3} + \frac{\partial^3 w}{R^2 \partial \theta^2 \partial x} \right) \right) \right) w dA, \quad (19)$$

where μ , ρ_E and v_x are viscosity, density and velocity of the fluid-nanoparticles, respectively. The fluid density and viscosity can be obtained by Mixture rule considering nanoparticles in the fluid as follows

$$\rho_f = \gamma \rho_{np} + (1 - \gamma) \rho_f, \quad (20)$$

$$\mu = (1 + 7.3\gamma + 123\gamma^2) \mu_f, \quad (21)$$

where ρ_f and ρ_{np} are respectively the density of the fluid and nanoparticles, μ_{np} and μ_f are respectively the viscosity of the fluid and nanoparticles and γ is the volume percent of the nanoparticles in the fluid.

2.4 Hamilton's principle

Applying Hamilton principle, the motion equations can be written as

$$\delta u : \frac{\partial N_{xx}}{\partial x} + \frac{\partial N_{x\theta}}{R \partial \theta} = I_0 \frac{\partial^2 u}{\partial t^2} + I_1 \frac{\partial^2 \phi_x}{\partial t^2}, \quad (22)$$

$$\delta v : \frac{\partial N_{x\theta}}{\partial x} + \frac{\partial N_{\theta\theta}}{R \partial \theta} + \frac{Q_\theta}{R} = I_0 \frac{\partial^2 v}{\partial t^2} + I_1 \frac{\partial^2 \phi_\theta}{\partial t^2}, \quad (23)$$

$$\delta w : \frac{\partial Q_x}{\partial x} + \frac{\partial Q_\theta}{R \partial \theta} - \frac{N_{\theta\theta}}{R} - k_w w + k_g \nabla^2 w - \rho_f A \left(\frac{\partial^2 w}{\partial t^2} + 2v_x \frac{\partial^2 w}{\partial x \partial t} + v_x^2 \frac{\partial^2 w}{\partial x^2} \right) + \mu A \left(\frac{\partial^3 w}{\partial x^2 \partial t} + \frac{\partial^3 w}{R^2 \partial \theta^2 \partial t} + v_x \left(\frac{\partial^3 w}{\partial x^3} + \frac{\partial^3 w}{R^2 \partial \theta^2 \partial x} \right) \right) = I_0 \frac{\partial^2 w}{\partial t^2}, \quad (24)$$

$$\delta \phi_x : \frac{\partial M_{xx}}{\partial x} + \frac{\partial M_{x\theta}}{R \partial \theta} - Q_x = I_2 \frac{\partial^2 \phi_x}{\partial t^2} + I_1 \frac{\partial^2 u}{\partial t^2}, \quad (25)$$

$$\delta \phi_\theta : \frac{\partial M_{x\theta}}{\partial x} + \frac{\partial M_{\theta\theta}}{R \partial \theta} - Q_\theta = I_2 \frac{\partial^2 \phi_\theta}{\partial t^2} + I_1 \frac{\partial^2 v}{\partial t^2}, \quad (26)$$

By integrating Eqs. (13) and (14) in the direction of thickness and using Eq. (8), the relationships of the forces and interior moments of the structure can be calculated as

$$N_{xx} = A_{110} \frac{\partial u}{\partial x} + A_{111} \frac{\partial \phi_x}{\partial x} + A_{120} \left(\frac{\partial v}{R \partial \theta} + \frac{w}{R} \right) + A_{121} \frac{\partial \phi_\theta}{R \partial \theta}, \quad (27)$$

where

$$(A_{11k}, A_{12k}, A_{22k}, A_{66k}) = \int_{-h/2}^{h/2} (C_{11}, C_{12}, C_{22}, C_{66}) z^k dz, \quad k = 0, 1, 2 \quad (35)$$

$$(A_{44}, A_{55}) = \int_{-h/2}^{h/2} (C_{44}, C_{55}) dz, \quad (36)$$

In this paper, three types of boundary conditions are used which are:

➤ **Simple-Simple (SS)**

$$x = 0, L \Rightarrow u = v = w = \phi_\theta = M_x = 0, \quad (37)$$

➤ **Clamped- Clamped (CC)**

$$x = 0, L \Rightarrow u = v = w = \phi_x = \phi_\theta = 0, \quad (38)$$

➤ **Clamped- Simple (CS)**

$$\begin{aligned} x = 0 &\Rightarrow u = v = w = \phi_x = \phi_\theta = 0, \\ x = L &\Rightarrow u = v = w = \phi_x = M_x = 0. \end{aligned} \quad (39)$$

3. DQ method

DQ is a numerical method which converts a differential equation to algebraic one using weighting coefficient. The main relationships of this method are expressed as the following (Madani *et al.* 2017, Shokravi 2017b)

$$\frac{d^n f_x(x_i, \theta_j)}{dx^n} = \sum_{k=1}^{N_x} A_{ik}^{(n)} f(x_k, \theta_j) \quad n = 1, \dots, N_x - 1. \quad (40)$$

$$\frac{d^m f_y(x_i, \theta_j)}{d\theta^m} = \sum_{l=1}^{N_\theta} B_{jl}^{(m)} f(x_i, \theta_l) \quad m = 1, \dots, N_\theta - 1. \quad (41)$$

$$\frac{d^{n+m} f_{xy}(x_i, \theta_j)}{dx^n d\theta^m} = \sum_{k=1}^{N_x} \sum_{l=1}^{N_\theta} A_{ik}^{(n)} B_{jl}^{(m)} f(x_k, \theta_l). \quad (42)$$

So, it is observed that Selection of the sample points and weighting coefficient are two very important factors in the DQ method. Chebyshev polynomial is widely used for solving the engineering problems as

$$X_i = \frac{L}{2} \left[1 - \cos \left(\frac{i-1}{N_x-1} \pi \right) \right] \quad i = 1, \dots, N_x \quad (43)$$

The weighting coefficient are generalized as below

a) for the first order derivative

$$A_{ij}^{(1)} = \begin{cases} \frac{M(x_i)}{(x_i - x_j)M(x_j)} & \text{for } i \neq j, \quad i, j = 1, 2, \dots, N_x \\ -\sum_{\substack{j=1 \\ i \neq j}}^{N_x} A_{ij}^{(1)} & \text{for } i = j, \quad i, j = 1, 2, \dots, N_x \end{cases} \quad (45)$$

$$B_{ij}^{(1)} = \begin{cases} \frac{P(\theta_i)}{(\theta_i - \theta_j)P(\theta_j)} & \text{for } i \neq j, \quad i, j = 1, 2, \dots, N_\theta \\ -\sum_{\substack{j=1 \\ i \neq j}}^{N_\theta} B_{ij}^{(1)} & \text{for } i = j, \quad i, j = 1, 2, \dots, N_\theta \end{cases} \quad (46)$$

where

$$M(x_i) = \prod_{\substack{j=1 \\ j \neq i}}^{N_x} (x_i - x_j) \quad (47)$$

$$P(\theta_i) = \prod_{\substack{j=1 \\ j \neq i}}^{N_\theta} (\theta_i - \theta_j) \quad (48)$$

b) for higher derivative

$$A_{ij}^{(n)} = n \left(A_{ii}^{(n-1)} A_{ij}^{(1)} - \frac{A_{ij}^{(n-1)}}{(x_i - x_j)} \right) \quad (49)$$

$$B_{ij}^{(m)} = m \left(B_{ii}^{(m-1)} B_{ij}^{(1)} - \frac{B_{ij}^{(m-1)}}{(\theta_i - \theta_j)} \right) \quad (50)$$

Using the following time modes, the terms with the time derivative are omitted and the differential equations will be entirely based on the local derivatives

$$d(x, y, t) = d_0(x, y) e^{\omega t}, \quad (51)$$

where ω refers to frequency and d shows the dynamic vector. Hence, the governing equations can be written as below in a matrix for

$$\left(\left[\underbrace{K_L + K_{NL}}_K \right] + \Omega [C] + \Omega^2 [M] \right) \begin{Bmatrix} \{d_b\} \\ \{d_d\} \end{Bmatrix} = 0, \quad (52)$$

in which $\Omega = \omega / h \sqrt{C_{11} / \rho}$ refers the dimensionless frequency. $[K_L]$, $[K_{NL}]$, $[C]$ and $[M]$ show the linear part of the stiffness matrix, the nonlinear part of the stiffness matrix, damper matrix and mass matrix, respectively. $\{d_b\}$ and $\{d_d\}$ are the dynamic range vectors in points of the boundary and domain. Based on eigenvalue problem, Eq. (52) can be written as

$$\begin{bmatrix} [0] & [I] \\ -[M^{-1}K] & -[M^{-1}C] \end{bmatrix} \{Z\} = \Omega \{Z\}, \tag{53}$$

in which $[I]$ shows the identity matrix and $[0]$ is the zero matrix.

4. Numerical results

In this section, the numerical results of the pipe conveying fluid-nanoparticles are presented. The pipe is made of Poly methyl methacrylate (PMMA) for the matrix which have constant Poisson's ratios of $\nu_m = 0.34$, temperature-dependent thermal coefficient of $\alpha_m = (1 + 0.0005\Delta T) \times 10^{-6} / K$, and temperature-dependent Young moduli of $E_m = (3.52 - 0.0034T) GPa$ in which $T = T_0 + \Delta T$ and $T_0 = 300 K$ (room temperature).

The density of the fluid (water) is $\rho_f = 998.2 Kg / m^3$ and its viscosity is $\mu_f = 1 \times 10^{-3} Pa.s$. The nanoparticles in the fluid is iron oxide with the density of $\rho_{np} = 3970 Kg / m^3$. Since the surrounding medium is relatively soft, the foundation stiffness k_w may be expressed by (Shen and Zhang 2011)

$$k_w = \frac{E_0}{4L(1-\nu_0^2)(2-c_1)^2} [5 - (2\gamma_1^2 + 6\gamma_1 + 5)\exp(-2\gamma_1)], \tag{54}$$

where

$$c_1 = (\gamma_1 + 2)\exp(-\gamma_1), \tag{55}$$

$$\gamma_1 = \frac{H_s}{L}, \tag{56}$$

$$E_0 = \frac{E_s}{(1-\nu_s^2)}, \tag{57}$$

$$\nu_0 = \frac{\nu_s}{(1-\nu_s)}, \tag{58}$$

where E_s , ν_s , H_s are Young's modulus, Poisson's ratio and depth of the foundation, respectively. In this paper, E_s is assumed to be temperature-dependent while ν_s is assumed to

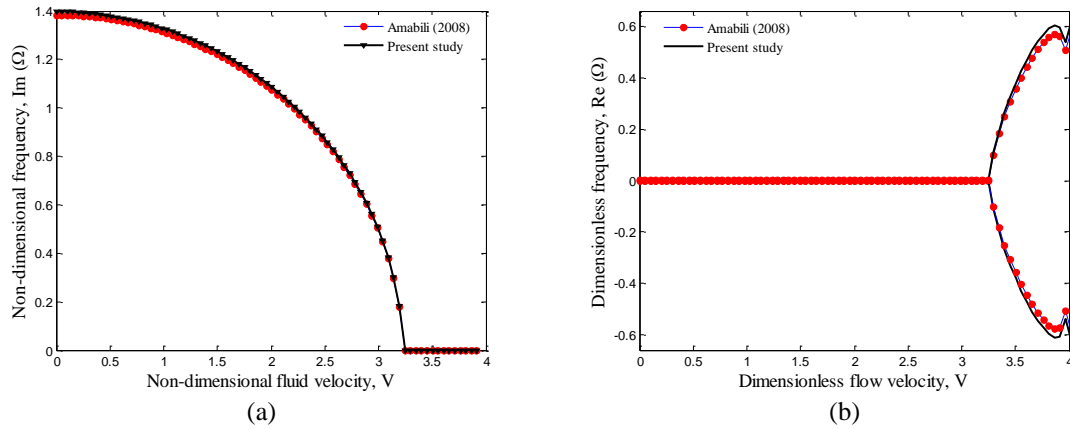


Fig. 2 Validation of present work (a) frequency and (b) damping

be a constant. The elastomeric medium is made of Poly dimethylsiloxane (PDMS) which the temperature-dependent material properties of which are assumed to be $\nu_s = 0.48$ and $E_s = (3.22 - 0.0034T)GPa$ in which $T = T_0 + \Delta T$ and $T_0 = 300 K$ (room temperature) (Shen and Zhang 2011).

4.1 Validation

In order to show the accuracy of the present work, neglecting the elastic medium and nanoparticles in the fluid, the results are compared with the work of Amabili (2008). However, considering a pipe with elastic modulus of $E = 206GPa$, Poisson's ratio of $\nu = 0.3$, density $\rho = 7850 Kg/m^3$, length to radius ratio of $L/R = 2$ and thickness to radius ratio of $h/R = 0.01$, the dimensionless frequency ($\Omega = \omega / \{\pi^2 / L^2 [D / \rho h]\}^{0.5}$) is plotted versus dimensionless fluid velocity ($V = v_x / \{\pi^2 / L [D / \rho h]\}^{0.5}$) in Fig. 2. As can be seen, present results agree well with the results of Amabili (2008).

4.2 Convergence of DQM

Fig. 3 shows the variation of dimensionless frequency ($\Omega = \omega / \{\pi^2 / L^2 [E_m / \rho_m]\}^{0.5}$) versus grid point number for different dimensionless fluid velocity ($V_x = v_x / \{\pi^2 / L [E_m / \rho_m]\}^{0.5}$). It can be seen that the dimensionless frequency is decreased with increasing the grid point number and for $N=15$, the results become converge.

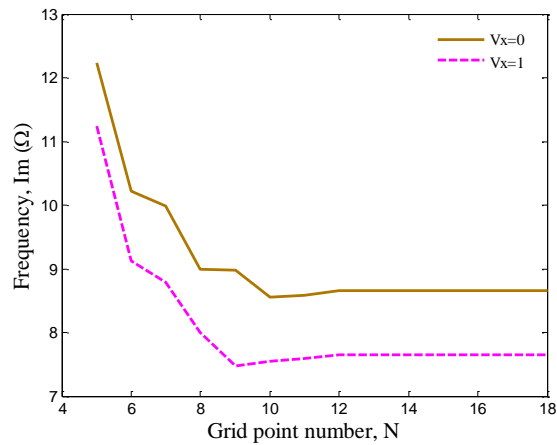


Fig. 3 Convergence and accuracy of DQM

4.3 The effect of the different parameters

In general, in all of the following figures, with increasing the fluid velocity, the frequency of the structure reduces until reaches to zero. In this state, the critical fluid velocity is happened. After the critical fluid velocity, the real part of frequency has two values of positive and negative which the positive one makes the structure divergence instable.

Fig. 4 illustrates the effect of nanoparticles volume percent on the dimensionless frequency and damping of the structure. A direct relationship can be fine between nanoparticles volume percent and frequency of the structure so that with increasing the nanoparticles volume percent, the dimensionless frequency and critical fluid velocity is increased. It is because with increasing the nanoparticles volume percent, the fluid velocity which leads to instability reduces.

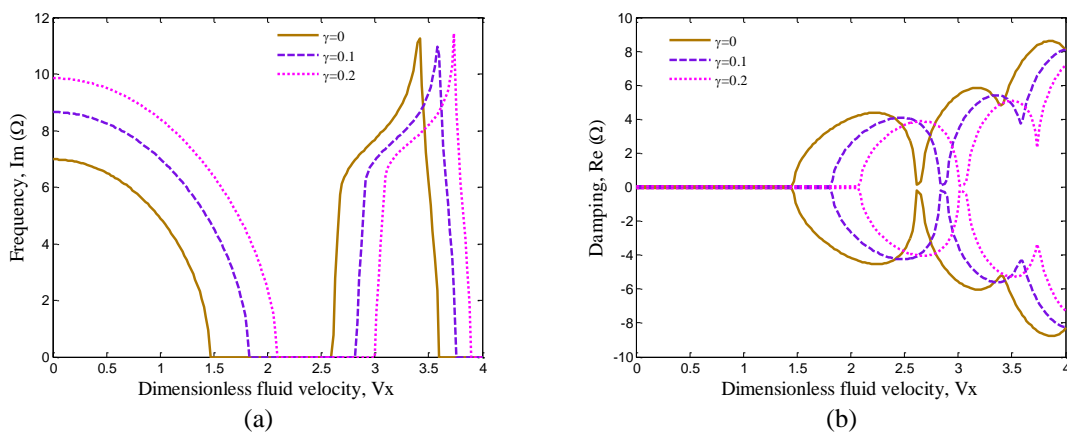


Fig. 4 The effect of volume percent of nanoparticles on the (a) frequency and (b) damping

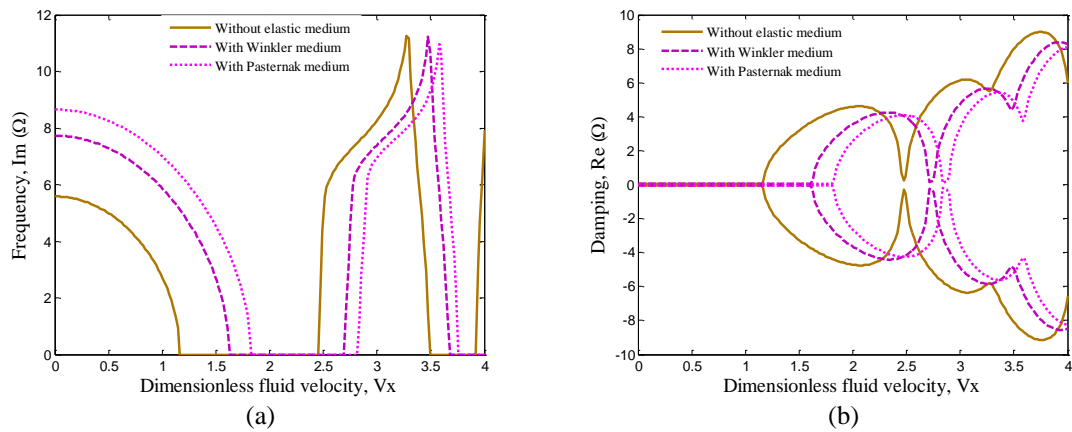


Fig. 5 The effect of elastic foundation on the (a) frequency and (b) damping

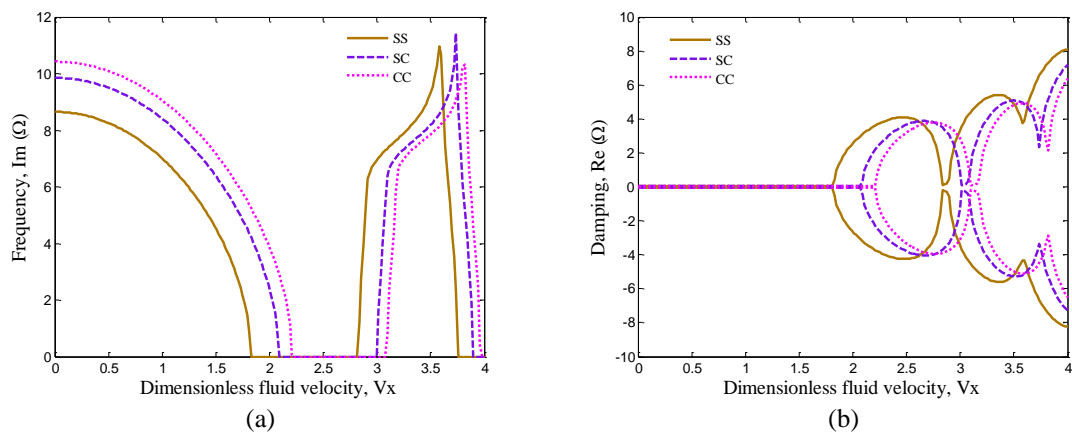


Fig. 6 The effect of different boundary conditions on the (a) frequency and (b) damping

The effect of the elastic medium on the dimensionless frequency and damping of the pipe versus the dimensionless fluid velocity is shown in Fig. 5. Three cases of without elastic medium, Winkler medium and Pasternak medium are considered. It can be find that considering elastic medium rises the dimensionless frequency and critical fluid velocity of the structure due to increase in the stiffness of the system. In addition, the dimensionless frequency and critical fluid velocity of cylindrical shell located in Pasternak medium are higher than that surrounded by Winkler foundation. It is due to this point that the Pasternak medium considers two elements of normal and shear forces.

Fig. 6 presents the effect of different boundary condition on the dimensionless frequency and damping of the pipe versus the dimensionless fluid velocity. It can be observed that the clamped-clamped (CC) boundary condition leads to higher dimensionless frequency and critical

fluid velocity with respect to other considered boundary conditions. It is due to the fact that the cylindrical shell with CC boundary condition has higher bending rigidity.

The temperature change effect on the dimensionless frequency and damping of the pipe versus the dimensionless fluid velocity is shown in Fig. 7. It can be concluded that with increasing the temperature change, the stiffness of cylindrical shell reduces and consequently, the dimensionless frequency and critical fluid velocity are decreased.

Fig. 8 demonstrates the effect of length to thickness ratio of the cylindrical shell on the dimensionless frequency and damping of the pipe against the dimensionless fluid velocity. As can be seen, with increasing the length to thickness ratio of the cylindrical shell, the dimensionless frequency and critical fluid velocity are decreased due to reduction in the stiffness of the structure.

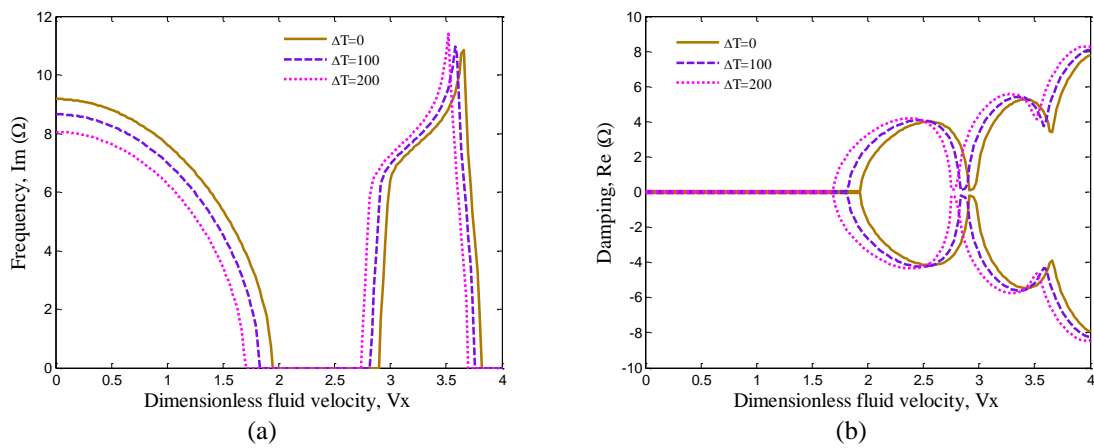


Fig. 7 The effect of temperature change on the (a) frequency and (b) damping

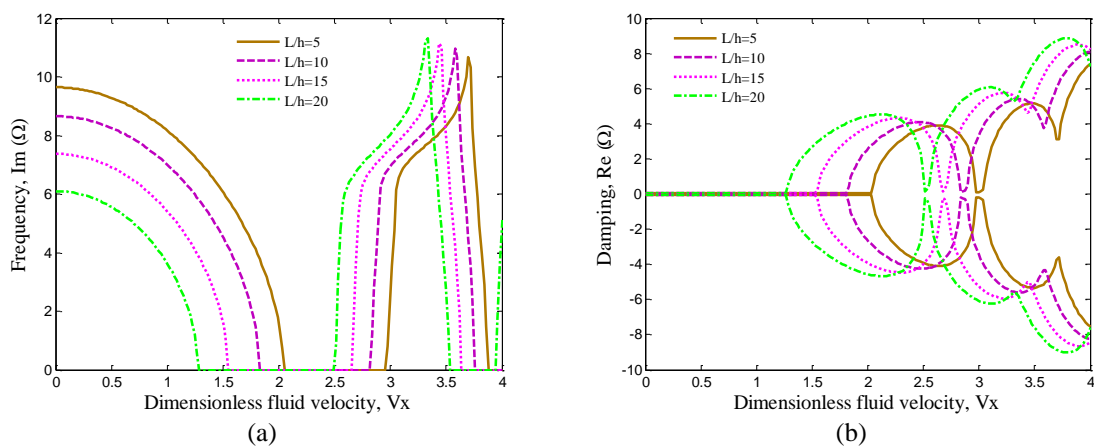


Fig. 8 The effect of length to thickness ratio of the cylindrical shell on the (a) frequency and (b) damping

5. Conclusions

In this work, vibration and instability of cylindrical shell conveying fluid mixed by nanoparticles were presented. The structure was surrounded by elastic foundation. The thermal load was considered and the structure was modeled by FSDT. Based on energy method and Hamilton's principle, the motion equations were derived and the effect of different parameters such as volume percent of nanoparticles, geometrical parameters of cylindrical shell, boundary condition, elastic medium and temperature change were considered. The most important findings of this paper were:

- ❖ With increasing the nanoparticles volume percent, the dimensionless frequency and critical fluid velocity was increased.
- ❖ It can be find that considering elastic medium rises the dimensionless frequency and critical fluid velocity of the structure due to increase in the stiffness of the system.
- ❖ The clamped-clamped (CC) boundary condition leads to higher dimensionless frequency and critical fluid velocity with respect to other considered boundary conditions.
- ❖ With increasing the temperature change, the stiffness of cylindrical shell reduces and consequently, the dimensionless frequency and critical fluid velocity were decreased.
- ❖ With increasing the length to thickness ratio of the cylindrical shell, the dimensionless frequency and critical fluid velocity were decreased.

References

- Amabili, M. (2008), *Nonlinear vibrations and stability of shells and plates*, New York, Cambridge University Press.
- Dai, H.L., Wang, L. and Ni, Q. (2013), "Dynamics of a fluid-conveying pipe composed of two different materials", *Int. J. Eng. Sci.*, **73**, 67-76.
- Deng, J., Liu, Y., Zhang, Z. and Liu, W. (2017), "Stability analysis of multi-span viscoelastic functionally graded material pipes conveying fluid using a hybrid method", *Eur. J. Mech. A - Solids*, **65**, 257-270.
- Ghaitani, M.M. and Majidian, A. (2017), "Frequency and critical fluid velocity analysis of pipes reinforced with FG-CNTs conveying internal flows", *Wind Struct.*, **24**(3), 267-285.
- He, T. (2015), "Partitioned coupling strategies for fluid-structure interaction with large displacement: Explicit, implicit and semi-implicit schemes", *Wind Struct.*, **20**(3), 423-448.
- Kutin, J. and Bajsić, I. (2014), "Fluid-dynamic loading of pipes conveying fluid with a laminar mean-flow velocity profile", *J. Fluid. Struct.*, **50**, 171-183.
- Maalawi, K.Y., Abouel-Fotouh, A.M., Bayoumi, M.El and Yehia, Kh.A.A. (2016), "Design of composite pipes conveying fluid for improved stability characteristics", *Int. J. Appl. Eng. Res.*, **11**(12), 7633-7639.
- Madani, H., Hosseini, H. and Shokravi, M. (2017), "Differential cubature method for vibration analysis of embedded FG-CNT-reinforced piezoelectric cylindrical shells subjected to uniform and non-uniform temperature distributions", *Steel Compos. Struct.*, **22**(4), 889-913.
- Marzani, A., Mazzotti, M., Viola, E., Vittori, P. and Elishakoff, I. (2012), "FEM formulation for dynamic instability of fluid-conveying pipe on nonuniform elastic foundation", *Mech. Based Des. Struct.*, **40**(1), 83-95.
- Ni, Q., Luo, Y., Li, M. and Yan, H. (2017), "Natural frequency and stability analysis of a pipe conveying fluid with axially moving supports immersed in fluid", *J. Sound Vib.*, **403**, 173-189.
- Ni, Q., Zhang, Z.L. and Wang, L. (2011), "Application of the differential transformation method to vibration analysis of pipes conveying fluid", *Appl. Math. Comput.*, **217**(16), 7028-7038.
- Qian, Q., Wang, L. and Ni, Q. (2009), "Instability of simply supported pipes conveying fluid under thermal

- loads”, *Mech. Res. Commun.*, **36**, 413-417.
- Reddy, J.N. (2004), *Mechanics of laminated composite plates and shells*, 2nd Ed., Washington, CRC press.
- Rivero-Rodriguez, J. and Pérez-Saborid, M. (2015), “Numerical investigation of the influence of gravity on flutter of cantilevered pipes conveying fluid”, *J. Fluid. Struct.*, **55**, 106-121.
- Ryu, B.J., Ryu, S.U., Kim, G.H. and Yim, K.B. (2004), “Vibration and dynamic stability of pipes conveying fluid on elastic foundations”, *KSME Int. J.*, **18**(12), 2148-2157.
- Shen, H.S. and Zhang, C.L. (2011), “Nonlocal beam model for nonlinear analysis of carbon nanotubes on elastomeric substrates”, *Comput. Mat. Sci.*, **50**(3), 1022-1029.
- Shokravi, M. (2017a), “Buckling analysis of embedded laminated plates with agglomerated CNT-reinforced composite layers using FSDT and DQM”, *Geomech. Eng.*, **12**, 327-346.
- Shokravi, M. (2017b), “Vibration analysis of silica nanoparticles-reinforced concrete beams considering agglomeration effects”, *Comput. Concrete*, **19**, 333-338.
- Sun, F.J. and Gu, M. (2014), “A numerical solution to fluid-structure interaction of membrane structures under wind action”, *Wind Struct.*, **19**(1), 35-58.
- Texier, B.D. and Dorbolo, S. (2015), “Deformations of an elastic pipe submitted to gravity and internal fluid flow”, *J. Fluid. Struct.*, **55**, 364-371.
- Wang, L. (2012), “Flutter instability of supported pipes conveying fluid subjected to distributed follower forces”, *Acta Mech. Solida Sin.*, **25**(1), 46-52.

